

K. Aydin* and J. Singh
 Pennsylvania State University, University Park, PA

1. INTRODUCTION

Millimeter wave radars operating at 95 GHz are being used for the remote sensing of ice clouds from airborne platforms for cloud microphysical studies and for understanding the effects of clouds on the Earth's radiation budget. 95-GHz polarimetric radars have the potential for identifying ice crystal types (Aydin and Singh, 2004) and for estimating bulk parameters such as ice water content (Aydin and Tang, 1997). Particle probe measurements in clouds show not only "pristine" or single type of ice crystals (e. g., hexagonal columns, hexagonal plates, stellar crystal, etc.) but also ice crystal aggregates and rimed crystals, which may be mixed with pristine crystals. This paper focuses on deriving polarimetric radar signatures of pristine ice crystals mixed with aggregates and rimed crystals. Radar signature simulations of these mixtures are compared with measurements and in situ particle probe images from field experiments conducted in 1997 in Wyoming (Wolde and Vali, 2001). These are unique experiments that provide simultaneous 95 GHz polarimetric radar data with particle probe measurements. Simulations and experimental data showed good agreement for the reflectivity factor (Z_h), differential reflectivity (Z_{DR}), and linear depolarization ratio (LDR).

Pristine crystals and their mixtures with aggregates and rimed crystals show different clustering characteristics on the $Z_h - Z_{DR}$, $Z_h - \text{LDR}$, and $Z_{DR} - \text{LDR}$ planes. An exception to this is the overlap of clustering patterns for columnar crystals and aggregates of stellar crystals and their rimed forms. A resolution for this problem is proposed using the clustering patterns of these crystals on the $Z_{DR} - \rho_{hv}$ plane, where ρ_{hv} is the correlation coefficient for copolarized signals. These results are expected to be useful in improving ice crystal classification algorithms based on 95 GHz polarimetric radar observables.

2. MODELS

The details for the stellar crystal models are given in earlier publications (Aydin and Walsh, 1999a,b). Here the modeling for aggregates and heavily rimed crystals including graupel-like snow is briefly described. These particles are modeled as oblate spheroids with axial ratios varying uniformly between 0.4 to 0.9. A Gaussian canting angle distribution is used for the polar canting (angle between the particle's symmetry axis and zenith) with 0° mean and 30° standard deviation to account for the wobbling motion of the particles as they fall. The

*Corresponding author address: Kultegin Aydin, Penn State Univ., Dept. of Electrical Engineering, University Park, PA, 16802; e-mail: k-aydin@psu.edu

azimuthal angle is assumed to be uniformly distributed between 0 and 2π .

Two different size-dependent density models were used. These are given by Mitchell et al. (1990) for heavily-rimed dendritic crystals and Brown and Francis (1995) for lower density crystals. In addition, two fixed-density models (0.2 g/cm^3 and 0.3 g/cm^3) were also considered. Here the results based on the density model from Mitchell et al. (1990) are presented. The Brown and Francis (1995) density model did not produce the observed ranges of values for the radar parameters considered in this study. The fixed density models produce results comparable to those presented here.

The size dependent density function of Mitchell et al. (1990) varies with the aspect ratio of the particles and for an oblate spheroid with an aspect ratio of 0.5 it is $0.216D^{-0.8} \text{ g/cm}^3$, where D is the equivalent-volume spherical diameter in mm units.

A gamma model size distribution, given by $N(D) = N_0 D^\mu \exp(-\lambda D)$, with D ranging from 0.1 to 6 mm is used. N_0 is left as a variable, and μ is varied incrementally between 0 and 2. The ice water content (IWC) is confined to the range 0.01 to 1 g/m^3 , and the total number of particles per unit volume is restricted to the range 0.01 to 50 per liter. The median mass volume is limited to less than 3 mm.

The mixing of stellar crystals with aggregates and rimed crystals are performed by considering different values of IWC in the range 0.06 to 0.8 g/m^3 . The stellar crystals are assumed to make up a certain percentage (e.g., 25%, 50%, etc.) of the IWC and the rest is due to the aggregates. A given IWC can be obtained from different size distributions, which lead to different reflectivities (Z_h). The chosen size distributions are those that produce Z_h values near its maximum, minimum and mean for the given IWC. These distributions also generate values for Z_{dr} and LDR_{hv} that cover their simulated ranges.

3. RESULTS AND DISCUSSIONS

Figure 1 shows scatter plots of polarimetric 95 GHz radar data obtained on 18 February 1997 during the WYICE'97 winter-spring campaign in Laramie, Wyoming. Figure 2 shows sample shadow images of ice crystals simultaneously obtained with particle probes on the University of Wyoming's King Air aircraft, which also housed the radar. The range resolution was 30 m (the closest resolution volume was 120 m from the radar) and aircraft speed 100 m s^{-1} . A two-gate running average (cross track) and a 0.6 second along track running average was performed on the data. The temperature during this penetration was -13.4° C .

The modeling results presented in Fig. 3 are to be compared with the data in Fig.1. It is clear that the ranges for Z_h (reflectivity factor), Z_{dr} (differential reflectivity), and LDR_{hv} (linear depolarization ratio) are very similar to the measurements in Fig.1. The part that is not similar is on the LDR_{hv} - Z_{dr} plane, where the LDR_{hv} is high and the Z_{dr} is low. The simulations do not show this. The combination of high LDR_{hv} and low Z_{dr} can be obtained by increasing the number of particles with smaller axial ratios and also increasing the canting angle standard deviation.

As noted earlier, the clustering patterns on the $Z_h - Z_{DR}$, $Z_h - LDR_{hv}$, and $Z_{DR} - LDR_{hv}$ planes for hexagonal columns is similar to those for mixtures of stellar crystals with aggregates and rimed crystals. Figure 4 shows simulated scatter plots of pairs of polarimetric radar observables including the correlation coefficient ρ_{hv} for hexagonal columns (Fig.4a) and mixtures of stellar crystals and aggregates and rimed crystals (Fig.4b). It is clearly seen from these simulations that the Z_{dr} - ρ_{hv} pair could be used for discriminating hexagonal columns from the mixture of crystals.

4. ACKNOWLEDGMENTS

Part of this research was supported by the National Science Foundation under grant ATM-9813512.

5. REFERENCES

- Aydin, K., and C. Tang, 1997: Relationships Between IWC and Polarimetric Radar Measurands at 94 and 220 GHz for Hexagonal Columns and Plates. *J. Atmos. Oceanic Technol.*, **14**, 1055-1063.
- Aydin, K., and T. M. Walsh, 1999: Millimeter wave scattering from spatial and planar bullet rosettes. *IEEE Trans. Geosci. Remote Sensing*, **37**(2), 1138-1150.
- Aydin, K., and J. Singh, 2004: Cloud Ice Crystal Classification Using a 95-GHz Polarimetric Radar. *J. Atmos. Oceanic Technol.*, **21**, 1679-1688.
- Brown, P., R., A., and P. N. Francis, 1995: Improved measurements of the ice water content in cirrus using a total-water probe. *J. Atmos. Oceanic Technol.*, **12**, 410-414.
- Mitchell, D. L., R. Zhang, and R. L. Pitter, 1990: Mass-dimensional relationships for ice particles and the influence of riming on snowfall rates. *J. Appl. Meteor.*, **29**, 153-163.
- Wolde, M., and G. Vali, 2001: Polarimetric signatures from ice crystals observed at 95 GHz in winter clouds. Part I: Dependence on crystal form. *J. Atmos. Sci.*, **58**, 828-841.

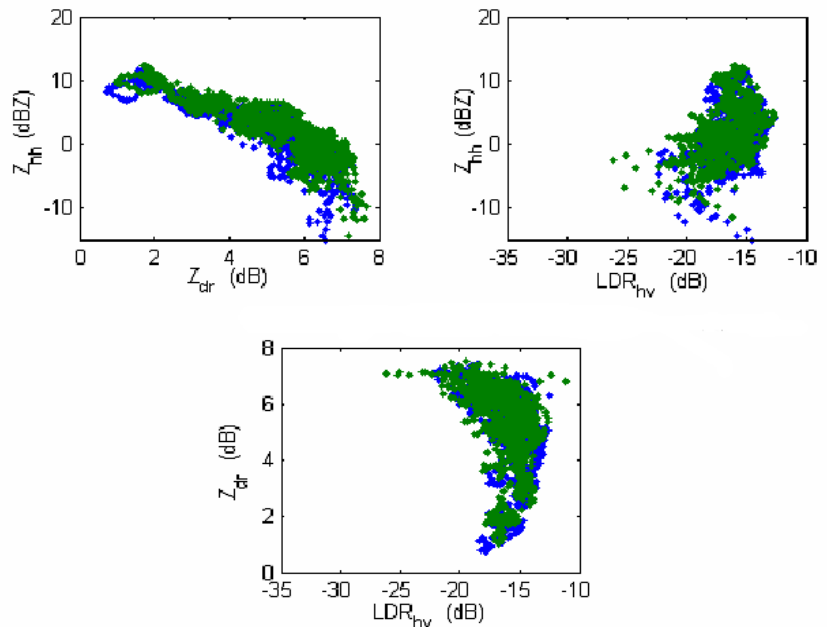


Fig. 1 Scatter plots of 95 GHz polarimetric radar observables from the 18 February, 1997 measurements, with the radar looking sideways. These correspond to the first two resolution volumes at 120 m and 150 m away from the radar.

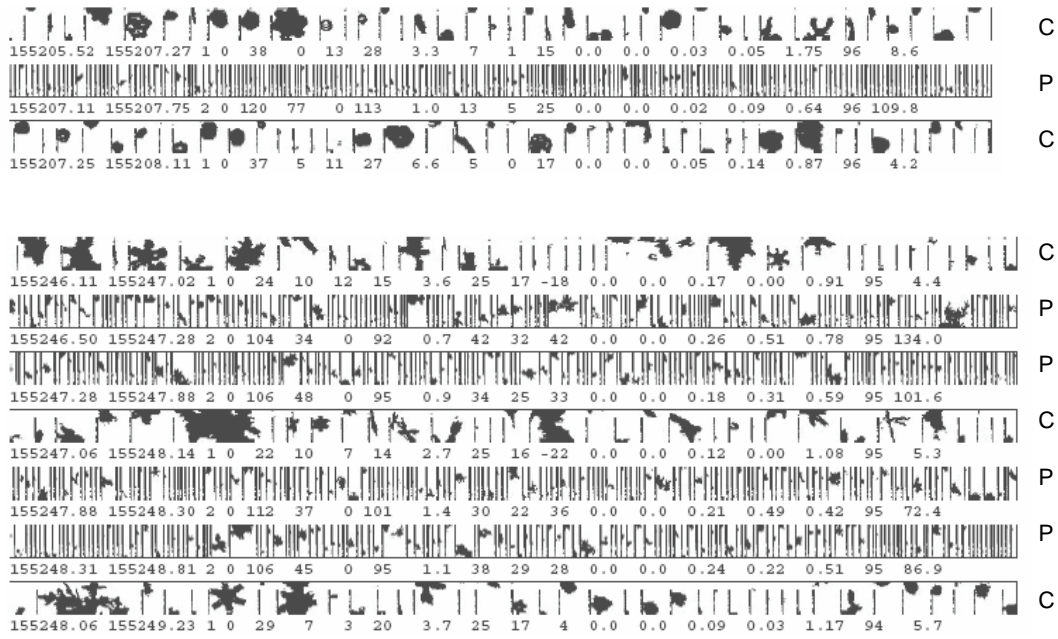


Fig. 2 Samples of particle probe shadow images obtained on 18 February, 1997 simultaneously with the radar data given in Fig.1 and within about 120 to 150 m apart in range. These are the particle probe images along the flight track. The P and C on the right side of the shadow images indicate that they are from the precipitation and cloud probes. The vertical lengths for the P and C probe images are 6.4 mm and 800 μm , respectively.

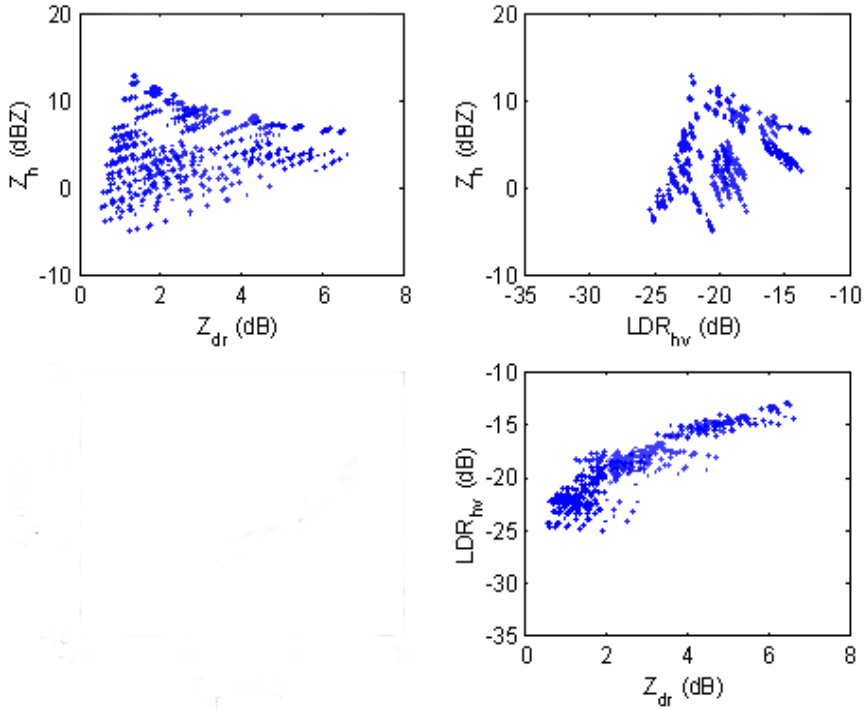
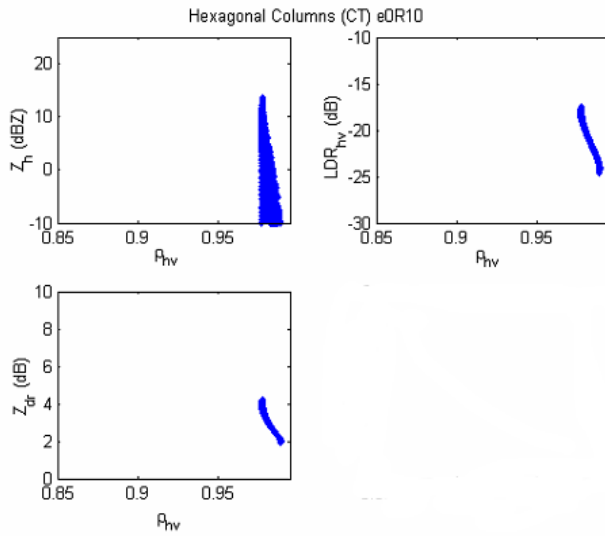
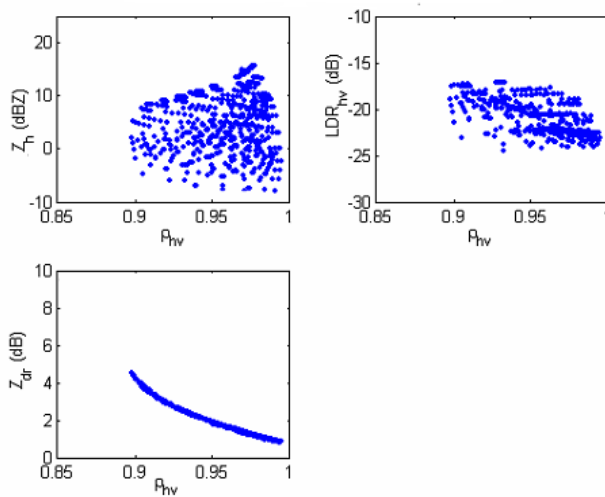


Fig. 3 Scatter plots of *simulated* 95 GHz polarimetric radar observables. Model details are in the text. This is a composite of results corresponding to stellar crystals making up 50%, 75%, and 90% of the total IWC in the mixture.



(a)



(b)

Fig. 4 Simulated scatter plots of polarimetric radar observables at 95 GHz for side incidence and corresponding to (a) hexagonal columns, and (b) mixtures of stellar crystals with aggregates and rimed crystals (this is a composite of results for stellar crystals making up 25% and 50% of the total IWC in the mixture).